Multiyear predictability of tropical marine productivity

Roland Séférian[a,b,1], Laurent Bopp[b], Marion Gehlen[b], Didier Swingedouw[b,c], Juliette Mignot[d,e], Eric Guilyardi[d,f], and Jérôme Servonnat[b]

[a]Centre National de Recherches Météorologiques–Groupe d'Etude de l'Atmosphère Météorologique/Groupe de Météorologie de Grande Echelle et Climat, 31100 Toulouse, France; [b]Institut Pierre Simon Laplace/Laboratoire des Sciences du Climat et de l'Environnement, 91191 Gif sur Yvette, France; [c]Université de Bordeaux/Environnements et Paléoenvironnements Océaniques et Continentaux, 33615 Pessac, France; [d]Institut Pierre Simon Laplace/Laboratoire d'Océanographie et du Climat: Expérimentations et Approches Numériques, 75252 Paris, France; [e]Climate and Environmental Physics, Physics Institute and Oeschger Centre of Climate Change Research, University of Bern, CH-3012 Bern, Switzerland; and [f]National Centre for Atmospheric Science Climate, University of Reading, Reading RG6 6BB, United Kingdom

Edited by David M. Karl, University of Hawaii, Honolulu, HI, and approved June 27, 2014 (received for review August 21, 2013)

With the emergence of decadal predictability simulations, research toward forecasting variations of the climate system now covers a large range of timescales. However, assessment of the capacity to predict natural variations of relevant biogeochemical variables like carbon fluxes, pH, or marine primary productivity remains unexplored. Among these, the net primary productivity (NPP) is of particular relevance in a forecasting perspective. Indeed, in regions like the tropical Pacific (30°N–30°S), NPP exhibits natural fluctuations at interannual to decadal timescales that have large impacts on marine ecosystems and fisheries. Here, we investigate predictions of NPP variations over the last decades (i.e., from 1997 to 2011) with an Earth system model within the tropical Pacific. Results suggest a predictive skill for NPP of 3 y, which is higher than that of sea surface temperature (1 y). We attribute the higher predictability of NPP to the poleward advection of nutrient anomalies (nitrate and iron), which sustain fluctuations in phytoplankton productivity over several years. These results open previously unidentified perspectives to the development of science-based management approaches to marine resources relying on integrated physical-biogeochemical forecasting systems.

forecast | ecosystem management | marine biogeochemistry

In 2010, global fisheries supplied the world with ∼148 million tons of fish with a total value of 217.5 billion US dollars (1). Fisheries represent a strong anthropogenic pressure on marine ecosystems and an increasing fraction of commercially exploited fish stocks are on the verge of collapse (1). However, in some oceanic regions like the tropical Pacific, which hosts the largest world fisheries (1), the decline of fish stocks cannot be attributed solely to overfishing. It is suspected to result from the interplay between human foraging and regional natural fluctuations in food abundance at the base of the food web such as variations in net primary productivity (NPP) occurring at interannual-to-decadal timescales. These natural fluctuations impact marine ecosystems across large oceanic regions (2). In the tropical Pacific, these fluctuations are suggested to be driven by large-scale climate variations such as the Madden Julian Oscillation (3), the El Niño Southern Oscillation (4), or the Pacific Decadal Oscillation (5). These climate modes are potentially predictable between one and up to several years (6, 7). However, although past studies have investigated the predictive skill of physical variables such as sea surface temperature (SST) (8) or precipitation (9) in the tropical Pacific, none has explored the potential predictability of natural variations of biogeochemical variables like NPP. This is all of the more surprising as the ability to predict natural variations of NPP at interannual-to-decadal timescales may be of key relevance to fisheries management (10–12).

Predicting Natural Variations of NPP

NPP is estimated from several algorithms on the basis of satellite-derived chlorophyll, SST, and photosynthetically available radiation (13). Continuous time series of satellite-derived estimates of NPP are available since 1997 based on products of the sea-viewing wide field-of-view sensor (SeaWiFS) (1997–2008) and the moderate-resolution imaging spectroradiometer (MODIS) (2003–2012). Despite substantial uncertainties in NPP mean state related to the different ocean color-based algorithms (14), the various algorithms show a good agreement for relative interannual-to-decadal variations (15). The overall spatial and temporal distributions of NPP are consistent with primary limitation by nutrients, and temperature (16), for which the largest interannual fluctuations are observed in the low-latitude oceans (17). Despite large differences in terms of spatial variability for NPP and SST in these regions, the temporal variations of NPP (with a SD of ∼120 $TgC{\cdot}mo^{-1}$) are tightly linked with low-latitude SST fluctuations, both being mainly associated to the El Niño Southern Oscillation (ENSO) variability (18). During ENSO phases, oscillations of NPP in the tropical Pacific prominently arise from changes in nutrient supply (4, 19, 20). In the eastern Pacific, the latter are injected from deeper layers to the upper ocean by the equatorial upwelling, the intensity of which is strongly modulated by changes in wind strength related to wind-SST Bjerknes feedbacks (21). In the central and western Pacific, the westward advection of nutrients in response to changes in zonal currents during the ENSO phases explains most of the variations in NPP with a time lag of several months (4, 20) to a decade (22, 23). Simultaneously to these first-order mechanisms, local limitation of specific nutrients plays an important role in setting the NPP variability. In particular, low iron levels are recognized to limit

Significance

Phytoplankton is at the base of the marine food web. Its carbon fixation, the net primary productivity (NPP), sustains most living marine resources. In regions like the tropical Pacific (30°N–30°S), natural fluctuations of NPP have large impacts on marine ecosystems including fisheries. The capacity to predict these natural variations would provide an important asset to science-based management approaches but remains unexplored yet. In this paper, we demonstrate that natural variations of NPP in the tropical Pacific can be forecasted several years in advance beyond the physical environment, whereas those of sea surface temperature are limited to 1 y. These results open previously unidentified perspectives for the future development of science-based management techniques of marine ecosystems based on multiyear forecasts of NPP.

Author contributions: R.S. designed research; R.S. performed research; R.S. analyzed data; L.B. and M.G. provided expertise on marine biogeochemistry; D.S., J.M., E.G., and J.S. provided expertise on decadal prediction; J.S. provided expertise on statistics; and R.S., L.B., M.G., D.S., J.M., E.G., and J.S. wrote the paper.

The authors declare no conflict of interest.

This article is a PNAS Direct Submission.

Freely available online through the PNAS open access option.

[1]To whom correspondence should be addressed. Email: roland.seferian@meteo.fr.

This article contains supporting information online at www.pnas.org/lookup/suppl/doi:10.1073/pnas.1315855111/-/DCSupplemental.

phytoplankton growth during the bloom (24), while high iron levels do not control the onset of the bloom (25). Earth system models (ESMs) that include a representation of the iron-nitrate colimitation within their ocean biogeochemical model reproduce the NPP–SST variations and processes linking changes in the physical ocean to ecosystem productivity (26). However, ESMs have so far never been used in seasonal-to-multiannual forecasting systems. Here, in the context of the recent "near-term" decadal Coupled Model Intercomparison Project Phase 5 (CMIP5) exercise (27), we use ensembles of predictions from the Institut Pierre Simon Laplace ESM, which all include an interactive ocean biogeochemistry (28).

Our study primarily aims at investigating the predictability of NPP and SST over the last two decades, covering the period of satellite ocean observations (1997–2008 and 2003–2011 for SeaWiFS and MODIS, respectively). We have focused our analysis on the 30°S–30°N tropical Pacific, because this region is located in the low-latitude permanently stratified waters and corresponds to some of the most productive open-ocean waters (18). We have restored SST anomalies of the ESM to the observations (29) from 1949 onward (this simulation, referred to as "nudged," is described in *SI Appendix*). The nudged simulation provides initial or starting conditions for a set of 10-y-long, three-member ensemble simulations for which SST restoring has been switched off. These simulations, referred to as "hindcasts," were started every year from 1987 to 2011 to cover the period of satellite observations (1997–2011). These simulations are used to assess the skill of retrospective prediction for NPP and SST, but also to attempt an experimental forecast the future evolution of NPP in the forthcoming decade (*SI Appendix*, Figs. S1 and S2).

Comparison between nudged and free (only forced by observed changes in atmospheric chemical composition, including volcanic impact, solar constant, and land use; *Methods*) ESM simulations clearly demonstrates that SST nudging improves the phasing and the amplitude of both SST and NPP interannual variability across the tropical Pacific compared to observations (Fig. 1 and *SI Appendix*, Fig. S4). Multiyear fluctuations of NPP and SST in the nudged simulation are both significantly correlated ($R > 0.6$) with observations at 95% confidence level.

The same variables in the free simulation show no significant correlation with the data, although external forcings like volcanic eruptions could partly ensure phasing between modeled and observed natural climatic fluctuations (28). In good agreement with previous studies, NPP anomalies are anticorrelated with SST anomalies, corresponding to the successive El Niño–La Niña climate state (18) (Fig. 1).

In our nudged experiments, these strong correlations illustrate that variations of simulated NPP are phased with those estimated from satellite measurements by our nudging strategy. However, only SST has been restored to the observations, and neither the wind nor the biological variables. Thus, NPP has been phased indirectly through dynamical and biogeochemical processes (*SI Appendix*, Fig. S5). Indeed, SST restoring induces a short-term dynamical adjustment of winds to the observed SST gradients. This dynamical adjustment improves the representation of zonal winds over a large fraction of the tropical Pacific with temporal correlation of >0.5 (significant at 90% confidence level) between modeled and satellite-derived zonal wind (*SI Appendix*, Fig. S3). The improved representation of the zonal wind pattern over the tropical Pacific ensures an accurate phasing of the eastern Equatorial upwelling with the various El Niño/La Niña events, and therefore the supply of nutrients available to phytoplankton growth (*SI Appendix* and *SI Appendix*, Figs. S6 and S7). Finally, as biological rates are directly affected by environmental temperature, SST restoring ensures the phasing of biological rates to the observed variability and thus improves the realism of the response of the NPP to the various El Niño/La Niña events.

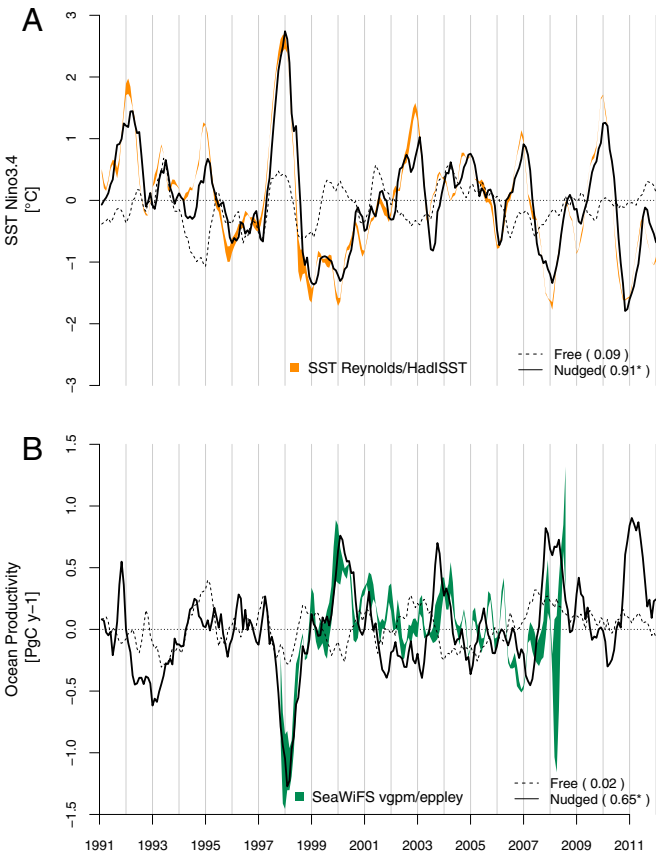

Fig. 1. Monthly detrended anomalies of (*A*) SST represented by the Nino3.4 index, (*B*) NPP integrated over the low-latitude Pacific ocean (30°S–30°N) from January 1991 to December 2011. Color shading for SST (in orange) and NPP (in green) denotes an evaluation of the differences between two observationally derived data products, which consists in the SD between the Reynolds and the HadISST reanalyses for SST and the Eppley–VGPM and the VGPM algorithm for NPP. The dashed lines indicate the free ESM simulation, whereas the bold lines indicate ESM simulations with SST nudging. Correlation between each ESM simulations compared with the SST reanalyses and the satellite-derived NPP are bracketed; correlations that pass a *t* test at 95% of significance following Bretherton et al. (44) are indicated by an asterisk (*).

We perform an evaluation of the predictive skill of our system using the hindcasts simulations over 1997–2011 for NPP and SST. The anomaly correlation skill score (AC-SS) between anomalies computed from the ensembles average of yearly-mean NPP and SST and the SST reanalyses and satellite-derived NPP provides a measure for evaluating the gain in skill attributable to nudging compared with the simulation starting from free conditions (30) (*SI Appendix*). In several regions, nudging initialization results in skillful prediction of natural variations in both NPP and SST 1 y in advance (Fig. 2 *A* and *D*). In the tropical Pacific, simulated NPP and SST variations closely follow observed ones with correlations of >0.6. The similarity between AC-SS for NPP and SST is lost for years 2–5 of the hindcasts (Fig. 2 *B* and *E*). At these lead times, our model still exhibits skill in predicting variations in NPP within the tropical Pacific, but not for those of SST (*SI Appendix*, Figs. S1 and S2).

Previous predictability studies completed AC-SS analysis with the root-mean-squared error skill score (RMSE-SS) to assess both phasing and divergence between mean trajectories of model ensembles and observations (31). Here, we use the combination of both measures in a single skill score diagram to diagnose the predictability horizon for both NPP and SST (Fig. 2 *C* and *F*). The predictability horizon (32) represents the time at which

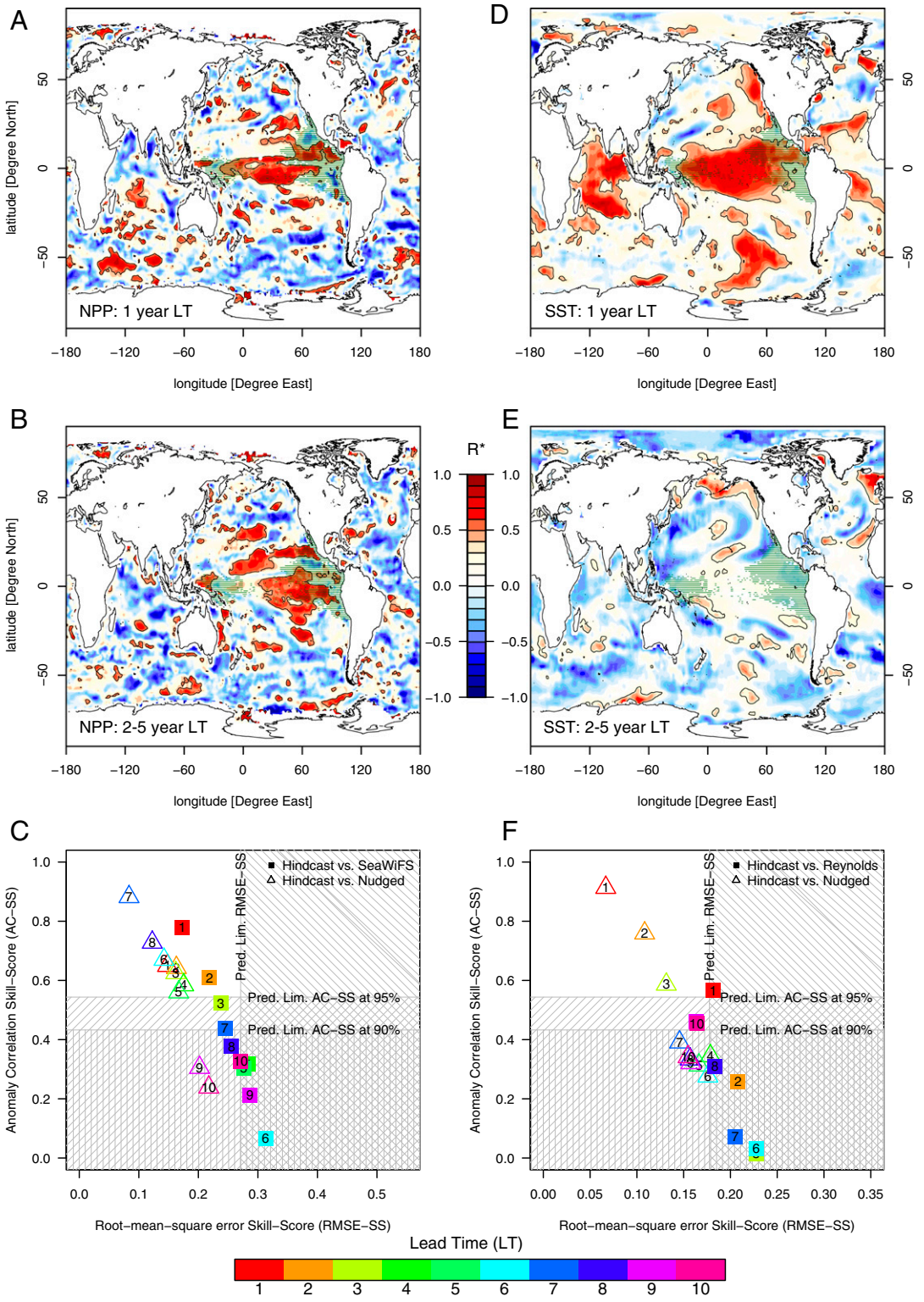

Fig. 2. Comparison of the predictive skill in reproducing observed variations in annual mean NPP and SST. (*A–C*) Correlation skill score in predicting estimated yearly mean anomalies of primary productivity of Eppley–VGPM and VGPM average. (*D–F*) SST (Reynolds and HadISST average). Skill at 1-y lead time (LT) of the hindcasts over the 10 y of SeaWiFS period for (*A*) the NPP and (*D*) the SST. As *A* and *D*, but over the lead time years 2–5 of the hindcasts for (*B*) the NPP and (*E*) the SST. Significance at 90% level confidence is contoured in black lines. Fishing areas from January 1991 to December 2011 within the low-latitude Pacific ocean (30°S–30°N) are indicated as green-hatched regions. Skill score diagram of the 10-y-long hindcasts evenly distributed over the SeaWiFS period (1998–2008) for (*C*) NPP and (*F*) the averaged SST within the low-latitude Pacific ocean. Both AC-SS and RMSE-SS are computed from yearly detrended anomalies over the SeaWiFS period (1998–2008) and over the MODIS period (2002–2012; *SI Appendix*, Fig. S11). The hatched regions indicate predictability limits at 90% and 95% for the AC-SS and the σ_{Obs} for the RMSE-SS. The filled squares and triangles indicate measures of effective and potential predictability, respectively. The numbers mentioned in both squares and triangles represent the lead time year (LT) of the hindcast prediction.

skillful prediction for a given variables is lost. It is defined here as the maximum lead time of the hindcasts for which AC-SS is significant at 90% and RMSE-SS is lower than the SD of the observations. The upper limit of the predictability horizon, referred to as potential predictability horizon, is obtained by considering a perfect nudging (33). It is derived from the comparison of hindcasts to the nudged simulation. Alternatively, comparing the hindcasts to the observations provides a more restrictive but unbiased estimate of the predictability horizon, referred to as the effective predictability horizon.

In the tropical Pacific, the effective predictability horizon for NPP extends up to 3 y, whereas that for SST hardly reaches 1 y (squares in Fig. 2 *C* and *F*). This result is corroborated by the analysis of the potential predictability horizon, which extends up to 8 y for NPP as opposed to 3 y for SST (triangles in Fig. 2 *C* and *F*). Additional experiments were performed to assess the robustness of the predictability horizon for NPP in a "perfect model framework" (*Methods* and *SI Appendix*). In this framework, we estimate the potential predictability horizon for NPP to be ~5.6 y in average across the various experiments, indicating that the 8-y-long predictability horizon is clearly the upper limit of predictability that can be expected from our model. The important difference in predictability horizon between NPP and SST translates into discrepancies in phasing and spread between the trajectories of hindcasts and observations. Although hindcast trajectories diverge substantially from the observed one after the first year of prediction for SST (normalized ensemble spread, >1), they closely follow the trajectory of the satellite-derived NPP up to 3 y in the case of NPP (normalized ensemble spread, ~0.5; *SI Appendix*, Fig. S1).

What Mechanisms or Properties Could Be Responsible for the Difference Between the SST and NPP Predictability Horizon?

Because phytoplankton growth is limited by nutrient availability in the tropical Pacific, we hypothesize that the propagation of nutrient anomalies pulsed by the successive ENSO events explains this difference in persistence over longer timescale. We assess this hypothesis by analyzing the persistence of anomalies of NPP, surface nutrients (nitrate and dissolved iron), and SST (Fig. 3), and the poleward propagation of NPP anomalies across the tropical Pacific (Fig. 4). The analysis of 5-y smoothed anomalies averaged across the tropical Pacific shows that persistence of NPP, estimated to 4 y, is comparable to that of surface nutrient anomalies. The persistence of both is larger than that of SST by a few years, suggesting that both NPP and surface nutrients exhibit a longer memory than SST.

The weaker persistence of SST anomalies reflects the tight coupling between SST and the lower atmosphere. SST anomalies are damped by heat exchange between the ocean and the atmosphere at short timescale (34). To the contrary, anomalies of nutrients and NPP evolve without direct interactions with the atmosphere. The absence of direct coupling between nutrients, as well as NPP and the atmosphere explains the longer persistence of their anomalies (Fig. 3). The persistence of salinity anomalies at interannual timescale (35) and their propagation across the Pacific at decadal timescales (36) have been previously ascribed to a similar mechanism. Our study suggests that, as for salinity, nutrient and NPP anomalies are transported by ocean currents across the tropical Pacific (Fig. 4). Spatial lagged correlation between the mixed layer and NPP demonstrates that NPP anomalies generated by ENSO-induced vertical supply of nutrients (Fig. 4*A*) are advected away from the equator over 1–5 y (Fig. 4 *B* and *C*). Such a trans-Pacific propagation of anomalies was proposed to drive the major differences in surface chlorophyll observed between 1997–1998 and 2009–2010 ENSO events (23).

Away from the region directly influenced by the upwelling, the persistence of NPP anomalies is partly modulated by biological processes because a fraction of nutrients is available to the phytoplankton growth through recycling of organic matter in the mixed layer (i.e., regenerated loop; *SI Appendix*). The influence of these processes on NPP variability and the resulting spatial repartition of regenerated versus new production (respectively in the western and eastern part of the tropical Pacific) are in agreement with previous regional modeling studies forced by atmospheric reanalyses (37, 38). Thus, the model predictive skill

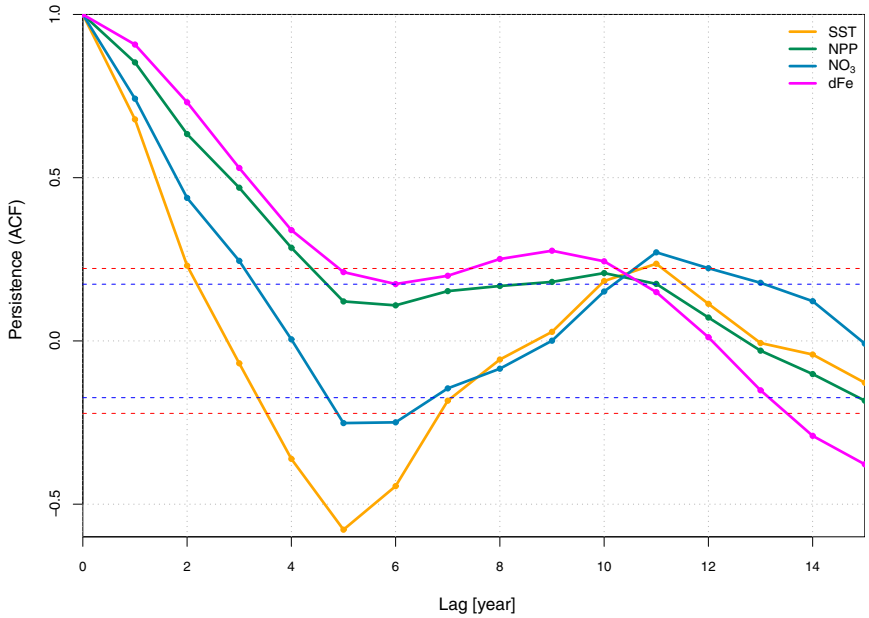

Fig. 3. Persistence of yearly anomalies for sea surface temperature (SST) and for surface concentrations of nitrate (NO_3), dissolved iron (dFe) averaged within 30°S–30°N Pacific and that of net primary productivity (NPP) integrated over the same latitudinal band in the nudged simulation. The null hypothesis of a zero correlation is tested against a *t* test at 90% and 95% significance levels. They are indicated in blue and red dashed lines, respectively. Persistences of yearly anomalies were computed from a 5-y running-mean smoothing over the 1991–2011 period.

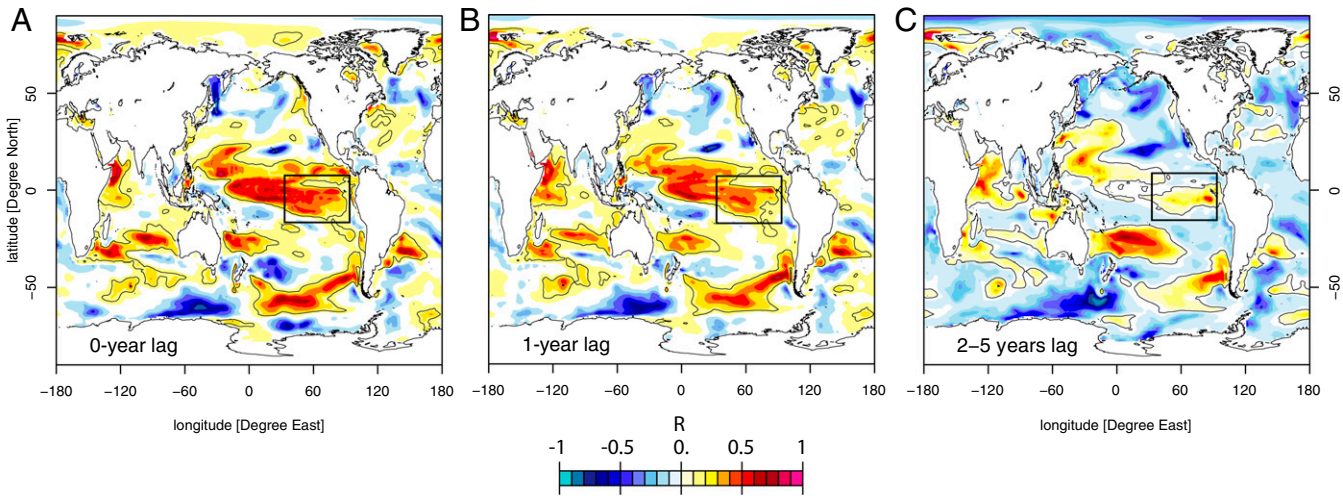

Fig. 4. Yearly correlation between the mixed layer depth at the location of its maximum (mentioned with the black box) and the NPP from January 1991 to December 2011 at (*A*) 0-y lag, (*B*) 1-y lag, and (*C*) averaged over the 2- to 5-y lags. Significance at 90% level confidence is contoured in black lines.

for nutrients and NPP benefits longer from SST nudging than SST itself, because nutrients are less directly affected by the stochastic forcing of the atmosphere (39).

Conclusions

In this first attempt to predict natural variations of NPP in the tropical Pacific, we demonstrate that NPP anomalies can be predicted up to 3 y in advance showing higher predictability than that of SST. Within this time frame, we can thus attempt to forecast future variations of NPP in the tropical Pacific. Our model predicts, with an agreement of five hindcasts over seven (~71%), an increase of NPP from 2013 to 2014 of 250 ± 200 TgC with a return to climatological values in 2015 (*SI Appendix*, Fig. S1).

Considering that skillful prediction of NPP was achieved through the nudging of SST only, our results open the perspective for future investigations of alternative nudging schemes including ocean color or hydrodynamical variables such as sea surface salinity. Benefits of such improved nudging were recently demonstrated for the realism of the Atlantic meridional overturning circulation (40). This approach holds thus the potential for an extension of the effective predictability horizon within the ultimate limit of our model set by the potential skill horizon of 8 y. Our results might prove useful for the management of fisheries across the tropical Pacific at interannual timescales. The combination of NPP monitoring as derived from satellite measurements and multiannual forecasts could be included to management strategies to adjust fishing pressure to natural climate variability. For the future development of integrated science-based management strategies for marine resources, our model skill will have to be compared with other forecast systems, pending of the inclusion of a fully interactive ocean biogeochemistry component. To ensure robust skill score statistics, the continuity of satellite ocean color measurements over the next decades is an essential requirement. Finally, the integrated end-to-end evaluation of the food chain needs still to be carried out to bridge the gap between NPP and fish biomass (12).

Methods

Data. This study relies on several datasets. Two datasets (29, 41) were used for SST to account for observational uncertainties in our skill score estimates. Similarly to SST, we used several estimates of NPP, which were derived from satellite measurements of SeaWiFS (1997–2008) and MODIS (2002–2012), along with vertically generalized production model (VGPM) (42) and Eppley–VGPM algorithms (13). These products are developed at the Oregon State University. Skipjack tuna catch biomass was estimated from purse seine data from 1991 to 2012 over the tropical Pacific (30°S–30°N). These data were provided by the Inter-American Tropical Tuna Commission (IATTC) and the Western and Central Pacific Fisheries Commission (WCPFC) for the Eastern and the Western part of the Pacific Ocean, respectively. Catch per units was combined onto a 1° × 1° regular Mercator grid (*SI Appendix*) and linearly detrended.

Simulations. Results of this study are based on simulations with the ESM developed at the Institut Pierre Simon Laplace (IPSL) for the CMIP5: IPSL-CM5A-LR (28). The following simulations were used in this study:

i) The free simulation corresponds to one member of the ensemble of historical simulations performed with IPSL-CM5A-LR for CMIP5. That is, between 1850 and 2005, the model is forced by observed changes in the atmospheric chemical composition, solar constant, and land use. From 2005 to 2011, IPSL-CM5A-LR is forced by changes in atmospheric chemical composition following the Representative Concentration Pathway 4.5 (RCP45).

ii) The nudged simulation results from the relaxation of observed SST anomalies to IPSL-CM5A-LR between 1949 and 2011 (28). Relaxation consists in adding a nudging term to the heat conservation equation at surface as follows:

$$\frac{\partial SST}{\partial t} = \ldots + \gamma_{nudg.}(SST_{ESM} - SST_{OBS}),$$

where the relaxation term, $\gamma_{nudg.}$, is $-40\ W{\cdot}m^{-2}{\cdot}K^{-1}$ is applied to the difference between the modeled and observed SST, SST_{ESM} and SST_{OBS}, respectively. It corresponds to a relaxing timescale of ~60 d for a mixed layer of 50-m depth.

iii) A set of 10-y-long, three-member ensemble hindcasts was performed every year between 1987 and 2001, covering the period from 1997 to 2011. They started from the initial or starting conditions provided by the nudged simulation for each three-member ensemble hindcast. There was no SST restoring during the 10 y of simulations for the hindcasts (meaning that the model was not guided by observed SST anomalies in these simulations). Hindcast ensembles were created by applying a white-noise perturbation on SST from the initial condition with an anomaly chosen randomly for each grid points in the interval ±0.05 °C.

iv) Several simulations are performed in a "perfect model framework" to conduct an in-depth evaluation of the NPP potential predictability skill scores. This experimental setup has been widely used and is detailed in ref. 43. The reference simulation consists in a 1,000-y-long preindustrial simulation of IPSL-CM5A-LR (1,800–2,799 in model years). Ten 20-y-long ensemble simulations were performed for five starting dates (i.e., 1,901, 2,056, 2,066, 2,071, and 2,171 in model years). At each starting date, these ensembles were generated with a similar perturbation method that used for generating the hindcasts.

Skill Scores. Skill scores were computed by comparing a time series constituted by the years of the hindcasts for a given lead time to that of the observations (*SI Appendix*). This methodology was used previously to assess benefits of SST nudging on North Atlantic region (30).

The AC-SS between model prediction (p) and observations (o) over N years was computed as follows:

$$\text{AC-SS} = \frac{1}{N} \frac{\sum (p-\overline{p})(o-\overline{o})}{\sum (p-\overline{p})^2 \sum (o-\overline{o})^2},$$

where the bar indicates the temporal averaging operator.

The significance of the AC-SS was tested against a two-tailed t test assuming $N - 2 - 1$ degree of freedom.

The RMSE-SS is given by the following:

$$\text{RMSE-SS} = \frac{1}{N} \sum [(p-\overline{p}) - (o-\overline{o})]^2.$$

The RMSE-SS was tested against the SD of the observations.

ACKNOWLEDGMENTS. We thank Dr. Philippe Ciais and Dr. Robert Vautard and the two anonymous reviewers for their useful comments on the paper. We also thank Mr. Peter G. Williams and Mr. Collin Millar from the Western and Central Pacific Fisheries Commission, as well as Dr. Guillermo Compean and Dr. Nick Vogel from the Inter-American Tropical Tuna Commission for their help with providing a tropical purse seine fishery dataset. This work was supported by Grand Equipement National de Calcul Intensif at Centre de Calcul Recherche et Technologie, Allocation 016178, and through the Groupe Mission Mercator Coriolis Projet en Partenariat Renforcé project "Green Mercator" by Centre National de la Recherche Scientifique Les Enveloppes Fluides et l'Environnement/Institut National des Sciences de l'Univers. This study also was partly funded by the Évaluation de la Prévisibilité Interannuelle à Décennale à Partir des Observations et des Modèles project (Gestion et Impacts du Changement Climatique) by the European Union project Seasonal-to-Decadal Climate Prediction for the Improvement of European Climate Services funded by the European Commission's Seventh Framework Research Program under Grant Agreement 243964.

1. Food and Agriculture Organization (2012) *The State of World Fisheries and Aquaculture—2012* (Fisheries and Aquaculture Department, Food and Agriculture Organization of the United Nations, Rome).
2. Chavez FP, et al. (1999) Biological and chemical response of the equatorial pacific ocean to the 1997-98 El Nino. *Science* 286(5447):2126–2131.
3. Waliser DE, Murtugudde R, Strutton P, Li J-L (2005) Subseasonal organization of ocean chlorophyll: Prospects for prediction based on the Madden-Julian Oscillation. *Geophys Res Lett* 32:L23602.
4. Messié M, Chavez FP (2012) A global analysis of ENSO synchrony: The oceans' biological response to physical forcing. *J Geophys Res* 117:C09001.
5. Martinez E, Antoine D, D'Ortenzio F, Gentili B (2009) Climate-driven basin-scale decadal oscillations of oceanic phytoplankton. *Science* 326(5957):1253–1256.
6. Chikamoto Y, Kimoto M, Ishii M, Mochizuki T (2013) An overview of decadal climate predictability in a multi-model ensemble by climate model MIROC. *Clim Dyn* 40: 1201–1222.
7. Wang B, et al. (2008) Advance and prospectus of seasonal prediction: Assessment of the APCC/CliPAS 14-model ensemble retrospective seasonal prediction (1980–2004). *Clim Dyn* 33:93–117.
8. Zwiers F (1996) Interannual variability and predictability in an ensemble of AMIP climate simulations conducted with the CCC GCM2. *Clim Dyn* 12:825–847.
9. Barlow M, Nigam S, Berbery EH (2001) ENSO, Pacific decadal variability, and US summertime precipitation, drought, and stream flow. *J Clim* 14:2105–2128.
10. Lehodey P, et al. (1998) Predicting skipjack tuna forage distributions in the equatorial Pacific using a coupled dynamical bio-geochemical model. *Fish Oceanogr* 7:317–325.
11. Chavez FP, Ryan J, Lluch-Cota SE, Niquen C M (2003) From anchovies to sardines and back: Multidecadal change in the Pacific Ocean. *Science* 299(5604):217–221.
12. Stock CA, et al. (2011) On the use of IPCC-class models to assess the impact of climate on Living Marine Resources. *Prog Oceanogr* 88:1–27.
13. Behrenfeld MJ (2005) Carbon-based ocean productivity and phytoplankton physiology from space. *Global Biogeochem Cycles* 19:GB1006.
14. Carr M-E, et al. (2006) A comparison of global estimates of marine primary production from ocean color. *Deep Sea Res Part II Top Stud Oceanogr* 53:741–770.
15. Henson SA, Raitsos D, Dunne JP, McQuatters-Gollop A (2009) Decadal variability in biogeochemical models: Comparison with a 50-year ocean colour dataset. *Geophys Res Lett* 36:L21601.
16. Field CB, Behrenfeld MJ, Randerson JT, Falkowski P (1998) Primary production of the biosphere: Integrating terrestrial and oceanic components. *Science* 281(5374): 237–240.
17. Behrenfeld MJ, et al. (2001) Biospheric primary production during an ENSO transition. *Science* 291(5513):2594–2597.
18. Behrenfeld MJ, et al. (2006) Climate-driven trends in contemporary ocean productivity. *Nature* 444(7120):752–755.
19. Rousseaux CS, Gregg WW (2012) Climate variability and phytoplankton composition in the Pacific Ocean. *J Geophys Res* 117:C10006.
20. Chavez FP, Messié M, Pennington JT (2011) Marine primary production in relation to climate variability and change. *Annu Rev Mar Sci* 3:227–260.
21. Bjerknes J (1969) Atmospheric teleconnections from the equatorial Pacific. *Mon Weather Rev* 97:163–172.
22. Rodgers KB, Aumont O, Menkes C, Gorgues T (2008) Decadal variations in equatorial Pacific ecosystems and ferrocline/pycnocline decoupling. *Global Biogeochem Cycles* 22:GB2019.
23. Gierach MM, Lee T, Turk D, McPhaden MJ (2012) Biological response to the 1997-98 and 2009-10 El Niño events in the equatorial Pacific Ocean. *Geophys Res Lett* 39: L10602.
24. Gordon RM, Coale KH, Johnson KS (1997) Iron distributions in the equatorial Pacific: Implications for new production. *Limnol Oceanogr* 42(3):419–431.
25. Gorgues T, et al. (2010) Revisiting the La Niña 1998 phytoplankton blooms in the equatorial Pacific. *Deep Sea Res Part I Oceanogr Res Pap* 57:567–576.
26. Schneider B, et al. (2008) Climate-induced interannual variability of marine primary and export production in three global coupled climate carbon cycle models. *Biogeosciences* 5:597–614.
27. Taylor KE, Stouffer RJ, Meehl GA (2011) An overview of CMIP5 and the experiment design. *Bull Amer Meteor Soc* 93:485–498.
28. Swingedouw D, Mignot J, Labetoulle S, Guilyardi E, Madec G (2013) Initialisation and predictability of the AMOC over the last 50 years in a climate model. *Clim Dyn* 40: 2381–2399.
29. Reynolds RW, Rayner NA, Smith TM, Stokes DC, Wang W (2002) An improved in situ and satellite SST analysis for climate. *J Clim* 15:1609–1625.
30. Keenlyside NS, Latif M, Jungclaus J, Kornblueh L, Roeckner E (2008) Advancing decadal-scale climate prediction in the North Atlantic sector. *Nature* 453(7191):84–88.
31. Kim H-M, Webster PJ, Curry JA (2012) Evaluation of short-term climate change prediction in multi-model CMIP5 decadal hindcasts. *Geophys Res Lett* 39:L10701.
32. Lorenz EN (1965) A study of the predictability of a 28-variable atmospheric model. *Tellus* 17:321–333.
33. Boer GJ, Kharin VV, Merryfield WJ (2013) Decadal predictability and forecast skill. *Clim Dyn* 41(7-8):1817–1833.
34. Frankignoul C (1985) Sea surface temperature anomalies, planetary waves, and air-sea feedback in the middle latitudes. *Rev Geophys* 23:357–390.
35. Mignot J, Frankignoul C (2003) On the interannual variability of surface salinity in the Atlantic. *Clim Dyn* 20:555–565.
36. Chen J, et al. (2014) Decadal modes of sea surface salinity and the water cycle in the tropical Pacific Ocean: The anomalous late 1990s. *Deep Sea Res Part I Oceanogr Res Pap* 84:38–49.
37. Wang XJ, Le Borgne R, Murtugudde R, Busalacchi AJ, Behrenfeld MJ (2008) Spatial and temporal variations in dissolved and particulate organic nitrogen in the equatorial Pacific: Biological and physical influences. *Biogeosciences* 5(6):1705–1721.
38. Wang XJ, Murtugudde R, Le Borgne R (2009) Nitrogen uptake and regeneration pathways in the equatorial Pacific: A basin scale modeling study. *Biogeosciences* 6(11):2647–2660.
39. Di Lorenzo E, Ohman MD (2013) A double-integration hypothesis to explain ocean ecosystem response to climate forcing. *Proc Natl Acad Sci USA* 110(7):2496–2499.
40. Servonnat J, et al. (2014) Reconstructing the subsurface ocean decadal variability using surface nudging in a perfect model framework. *Clim Dyn*, 10.1007/s00382-014-2184-7.
41. Rayner NA, et al. (2003) Global analyses of sea surface temperature, sea ice, and night marine air temperature since the late nineteenth century. *J Geophys Res* 108(D14): 4407.
42. Behrenfeld MJ, Falkowski PG (1997) Photosynthetic rates derived from satellite-based chlorophyll concentration. *Limnol Oceanogr* 42:1–20.
43. Persechino A, Mignot J, Swingedouw D, Labetoulle S, Guilyardi E (2013) Decadal predictability of the Atlantic meridional overturning circulation and climate in the IPSL-CM5A-LR model. *Clim Dyn* 40:2359–2380.
44. Bretherton CS, Widmann M, Dymnikov VP, Wallace JM, Bladé I (1999) The effective number of spatial degrees of freedom of a time-varying field. *J Climate* 12(7): 1990–2009.